Effects of self-fields on electron trajectory and gain in planar wiggler free-electron lasers with two-stream and ion-channel guiding

S. Saviz† and M. Karimi

Plasma Physics Research Center, Science and Research Branch, Islamic Azad University, Tehran, P. O. Box 14665-678, *Iran*

(Received 30 July 2013; revised manuscript received 21 August 2013; published online 24 January 2014)

The effects of self-fields on electron trajectories and gain in planar wiggler free-electron lasers with two-stream and ion-channel guiding are investigated. An analysis of the two-stream quasi-steady-state electron trajectories is given by solving the equation of motion in the presence of ion-channel guiding and the planar wiggler. The electron trajectories and the gain are derived. The stability of the trajectories, the characteristics of the linear gain, and the normalized maximum gain are studied numerically. The numerical calculations show that there are eight group trajectories rather than the two groups reported in the absence of the self-fields. It is also shown that the normalized gain group seven (G7) decreases while the rest increases with the increase in normalized ion-channel frequency. The two-stream instability and the self-field lead to a decrease in the maximum gain, except for G7.

Keywords: two-stream free-electron laser

PACS: 41.60.Cr

DOI: 10.1088/1674-1056/23/3/034103

1. Introduction

The free-electron laser is a high-power, continuously tunable source of coherent electromagnetic radiation that uses a beam of relativistic electrons passing through a long, transverse magnetic field to amplify electromagnetic radiation.[1–5] Ion-channel guiding of the relativistic electron beam in a free-electron laser (FEL) attracted attention as an alternative to guiding using a solenoid magnetic field after it was first proposed for use in a FEL by Takayama and Hirumatsu.[6] In recent years, the ion-channel guiding technique has emerged as an effective method for focusing relativistic electron beams in accelerators and FELs.[7]

The first-order self-magnetic field generated by wiggler-induced transverse velocity was calculated by Freund *et al.*[8] Recently, more exact calculations of self-fields and analysis of their effects on electron orbits have been published.[9,10] Esmaeilzadehand *et al.*[11] found small signal gain in a planar wiggler with ion-channel guiding when the self-fields are negligible. Farokhiand *et al.*[12] showed the self-field effects in FELs with a planar wiggler and ion-channel guiding on the quasi-steady-state orbits and the gain.

McNeil *et al.*[13] investigated a model of a FEL amplifier wiggler operating simultaneously with two electron beams of different energies in a planar wiggler. Bekefi and Jacobs[14] showed that the injection of the pre-bunched streams into a static, periodic wiggler enhances the intensity of the parametrically excited, backscattered electromagnetic wave. The effect of two-stream instability on the growth rate of FELs with an axial guide field was investigated in Refs. [15] and [16]. Saviz *et al.*[17] found that the two-stream with ion-channel field enhances the maximum gain in comparison with that for a single beam.

The purpose of this paper is to investigate the effects of self-fields on electron trajectory and gain in a two-stream FEL with planar wiggler and ion-channel guiding. The paper organized as follows. In Section 2, the single-particle trajectories of two streams in the presence of ion-channel guiding and self-fields are analyzed, and stability analysis of the steady-state trajectories is performed. In Section 3, we find the gain equation for a two-stream FEL with a planar wiggler and ion-channel guiding when self-fields are included. Finally, the numerical results and conclusions are given in Section 4.

2. Single-particle orbits

The physical configuration consists of a two-stream relativistic electron beam propagating through a planar wiggler in the presence of ion-channel guiding. The planar wiggler magnetic field is described by

$$\boldsymbol{B}_{\rm w} = B_{\rm w}\hat{e}_y \sin k_{\rm w} z, \tag{1}$$

where $k_{\rm w} = 2\pi/\lambda_{\rm w}$ is the wiggler wave number and $\lambda_{\rm w}$ is the wiggler wavelength. The transverse electrostatic field generated by an ion-channel guiding can be written as

$$\boldsymbol{E}_{\rm i} = 2\pi e n_{\rm i}\,(x\hat{e}_x + y\hat{e}_y)\,, \tag{2}$$

where $n_{\rm i}$ is the density of positive ions with charge e. The equilibrium self-electric and self-magnetic fields of the beams are

$$E_{\rm s} = -2\pi e \sum_{j=1}^{2} n_{{\rm b}j}(x\hat{e}_x + y\hat{e}_y), \tag{3}$$

$$B_{\rm s} = 2\pi e \sum_{j=1}^{2} n_{{\rm b}j}\beta_{zj}\,[y\hat{e}_x - x\hat{e}_y]. \tag{4}$$

†Corresponding author. E-mail: Shahrooz.saviz@srbiau.ac.ir

© 2014 Chinese Physical Society and IOP Publishing Ltd

The relativistic equations of motion for an electron with rest mass m and charge $-e$ moving with velocity $\boldsymbol{v}$ in these combined fields are

$$\frac{\mathrm{d}}{\mathrm{d}t}(m\gamma_j \boldsymbol{V}_j) = -e\left[\boldsymbol{E}_\mathrm{i} + \boldsymbol{E}_\mathrm{s} + \frac{1}{c}\boldsymbol{V}_j \times (\boldsymbol{B}_\mathrm{w} + \boldsymbol{B}_\mathrm{s})\right], \quad (5)$$

where γ_j is the relativistic factor, and c is the speed of light in a vacuum. With the aid of Eq. (5) and fields (1)–(4), the normalized constant transverse velocity of each beam is given by

$$\beta_{xj} = \frac{\bar{\Omega}_{\mathrm{w}j}\beta_{zj}^2}{\bar{\omega}_{ij}^2 - \sum_{j=1}^{2}\bar{\omega}_{\mathrm{b}j}^2 + \beta_{zj}\sum_{j=1}^{2}\bar{\omega}_{\mathrm{b}j}^2\beta_{zj} - \beta_{zj}^2}, \quad j = 1,2, \quad (6)$$

$$\beta_{yj} \cong 0, \quad j = 1,2, \quad (7)$$

$$\beta_{zj} = \text{const}, \quad j = 1,2, \quad (8)$$

where

$$\bar{\omega}_{\mathrm{b}j}^2 = \frac{2\pi e^2 n_\mathrm{b}}{\gamma_j m\, ck_\mathrm{w}}, \quad \bar{\omega}_{ij}^2 = \frac{2\pi e^2 n_j}{\gamma_j m\, ck_\mathrm{w}},$$

and

$$\bar{\Omega}_{\mathrm{w}j} = \frac{eB_\mathrm{w}}{\gamma_j mc\, ck_\mathrm{w}}$$

note the normalized beam frequency, the normalized ion-channel frequency, and the normalized wiggler frequency, respectively. The stability of the orbits can be determined by applying small perturbations to the steady-state orbits. To investigate the orbital stability, we assume $x_j = x_j + \delta x_j$, $y_j = \delta y_j$, $v_{xj} = v_{xj} + \delta v_{xj}$, $v_{yj} = \delta v_{yj}$, $v_{zj} = v_{zj} + \delta v_{zj}$, where $j = 1,2$. The orbit equations for each of the streams are

$$\delta\ddot{x} = -P_j\delta x_j + \Omega_{\mathrm{w}j}\sin(k_{\mathrm{w}j}z_j)\delta\dot{z}, \quad (9)$$

$$\delta\ddot{z}_j = A_j\beta_{xj}\delta x_j - M_i\delta\dot{x}_j, \quad (10)$$

where the dots represent differentiation with respect to time. By eliminating δz_j between Eqs. (9) and (10), we have

$$M_j\delta\dddot{x}_j - \dot{M}_j\delta\ddot{x}_j + A_j\delta\dot{x}_j - B_j\delta x_j = 0, \quad (11)$$

where

$$P_j = \omega_{ij}^2 - \sum_{j=1}^{2}\omega_{\mathrm{b}j}^2 + \beta_{zj}\sum_{j=1}^{2}\omega_{\mathrm{b}j}^2\beta_{zj}, \quad T_j = \sum_{j=1}^{2}\omega_{\mathrm{b}j}^2\beta_{zj},$$

$$M_j = \Omega_{\mathrm{w}j}\sin(k_{\mathrm{w}j}z_j) - \frac{x_j}{c}\sum_{j=1}^{2}\omega_{\mathrm{b}j}^2\beta_{zj},$$

$$A_j = M_j^3 + P_jM_j,$$

$$\dot{M}_j = \Omega_{\mathrm{w}j}\beta_{zj}\cos(k_{\mathrm{w}j}z_j) - \beta_{xj}\sum_{j=1}^{2}\omega_{\mathrm{b}j}^2\beta_{zj},$$

$$B_j = M_j^2\beta_{xj}\sum_{j=1}^{2}\omega_{\mathrm{b}j}^2\beta_{zj} + P_j\dot{M}_j.$$

We assume that all the variables oscillate with the same frequency ω, e.g.,

$$\delta x_j \approx \exp(\mathrm{i}\omega t).$$

Using the above assumption, Eq. (11) becomes

$$\overline{M_j^2}\bar{\omega}^3 + \overline{(\dot{M}_j^2 + 2A_jM_j)}\bar{\omega}^2 + \overline{(A_j^2 + 2\dot{M}_jB_j)}\bar{\omega} + \overline{B_j^2} = 0, \quad (12)$$

where $\bar{\omega} = \omega^2$. This equation has three roots for $\bar{\omega}$. The stability of the quasi-steady-state two-stream electron trajectory requires that these roots, $\bar{\omega}_1$, $\bar{\omega}_2$, and $\bar{\omega}_3$, are real and positive.

3. Small-signal gain

Consider the electromagnetic radiation co-propagating with the electron in the FEL interaction region. The electric and magnetic fields of the radiation with circular polarization may be represented by

$$\boldsymbol{E}_{rj} = E_{rj}\{\cos(\xi)\hat{e}_x - \sin(\xi)\hat{e}_y\}, \quad (13)$$

$$\boldsymbol{B}_{rj} = B_{rj}\{\sin(\xi)\hat{e}_x - \cos(\xi)\hat{e}_y\}, \quad (14)$$

where $\xi = k_rz - \omega_rt + \varphi$ is the phase, k_r is the wave number and ω_r is the angular frequency.

The energy exchange of the electron with the radiation field is given by

$$\frac{\mathrm{d}\gamma_j}{\mathrm{d}t} = -\frac{e}{m_\mathrm{e}c}\boldsymbol{\beta}_j\cdot\boldsymbol{E}_j = -\frac{e}{m_\mathrm{e}c}(\beta_{xj}\cos\xi - \beta_{yj}\sin\xi). \quad (15)$$

Substituting equations (7) and (8) into Eq. (15) yields

$$\begin{aligned}\frac{\mathrm{d}\gamma_j}{\mathrm{d}t} &= -\frac{eE_{rj}}{m_\mathrm{e}c}\frac{\bar{\Omega}_{\mathrm{w}j}\beta_{zj}^2}{\bar{\omega}_{ij}^2 - \sum_{j=1}^{2}\bar{\omega}_{\mathrm{b}j}^2 + \beta_{zj}\sum_{j=1}^{2}\bar{\omega}_{\mathrm{b}j}^2\beta_{zj} - \beta_{zj}^2} \\ &\quad\times\cos(k_\mathrm{w}z_j)\cos\xi \\ &= \frac{eE_{rj}}{m_\mathrm{e}c}\frac{\bar{\Omega}_{\mathrm{w}j}\beta_{zj}^2}{\bar{\omega}_{ij}^2 - \sum_{j=1}^{2}\bar{\omega}_{\mathrm{b}j}^2 + \beta_{zj}\sum_{j=1}^{2}\bar{\omega}_{\mathrm{b}j}^2\beta_{zj} - \beta_{zj}^2} \\ &\quad\times[\cos(k_{\mathrm{w}j}z_j + \xi) + \cos(k_{\mathrm{w}j}z_j - \xi)]. \end{aligned} \quad (16)$$

Let the electron phase be defined as

$$\psi \equiv (k_r + k_\mathrm{w})z - \omega_rt + \frac{\pi}{2} + \phi. \quad (17)$$

By using the first-order approximation, in $\xi = k_rz - \omega_rt + \varphi$, and considering the synchronism condition, i.e., $\Omega \equiv (k_\mathrm{w} + k_r)c\beta_{zj} - \omega_r \approx 0$, Eq. (16) can be written as

$$\begin{aligned}\frac{\mathrm{d}\gamma_j}{\mathrm{d}t} &= -\frac{eE_{rj}}{m_\mathrm{e}c}\frac{\bar{\Omega}_{\mathrm{w}j}\beta_{zj}^2}{\bar{\omega}_{ij}^2 - \sum_{j=1}^{2}\bar{\omega}_{\mathrm{b}j}^2 + \beta_{zj}\sum_{j=1}^{2}\bar{\omega}_{\mathrm{b}j}^2\beta_{zj} - \beta_{zj}^2} \\ &\quad\times\cos(\Omega t + \varphi), \end{aligned} \quad (18)$$

where the synchronism condition means that the electrons are near resonance with the wave. The φ phase in the above equation determines the initial position of the electron relative to the optical wave. Assume that $z_j(t) = c\beta_{zj}t + c\int\Delta\beta_{zj}(t')\mathrm{d}t'$. Substituting the root-mean-square value of the transverse velocity components into $\gamma_j^{-2} = 1 - \beta_{xj}^2 - \beta_{yj}^2 - \beta_{zj}^2$ gives an expression for the normalized axial velocity β_{zj}, which may be expanded for $\gamma \gg 1$ and β_{zj} close to 1 to obtain

$$\beta_{zj} = 1 - \frac{1}{2\gamma_j^2}\left(1 + \frac{\bar{\Omega}_{wj}^2 \beta_{zj}^4 \gamma_j^2}{2(\bar{\omega}_{ij}^2 - \sum_{j=1}^{2} \bar{\omega}_{bj}^2 + \beta_{zj}\sum_{j=1}^{2} \bar{\omega}_{bj}^2 \beta_{zj} - \beta_{zj}^2)^2}\right). \quad (19)$$

By differentiating Eq. (19) with respect to time and using Eq. (18), we obtain the following equation

$$z_j(t) = v_{zj}t + \frac{cD}{\Omega^2}\left[\cos(\Omega t + \varphi) - \cos\varphi + \Omega t \sin\varphi\right], \quad (20)$$

where

$$D = \frac{eE_{rj}}{2mc\gamma^3}\left(\frac{\bar{\Omega}_w \beta_{zj}^2}{\omega_{ij}^2 - \sum_{j=1}^{2} \omega_{bj}^2 + \beta_{zj}\sum_{j=1}^{2} \omega_{bj}^2 \beta_{zj} - \beta_{zj}^2}\right) \times \left(1 - \frac{\bar{\Omega}_{wj}^2 \beta_{zj}^2}{(\bar{\omega}_{ij}^2 - \sum_{j=1}^{2} \bar{\omega}_{bj}^2 + \beta_{zj}\sum_{j=1}^{2} \bar{\omega}_{bj}^2 \beta_{zj} - \beta_{zj}^2)^3}\right).$$

Substituting Eq. (20) into Eq. (16) and averaging over all phases φ leads to

$$\left\langle \frac{d\gamma_j}{dt} \right\rangle_\varphi = \frac{eE_{rj}}{4mc} \frac{\bar{\Omega}_{wj}\beta_{zj}^2}{(\bar{\omega}_{ij}^2 - \sum_{j=1}^{2} \bar{\omega}_{bj}^2 + \beta_{zj}\sum_{j=1}^{2} \bar{\omega}_{bj}^2 \beta_{zj} - \beta_{zj}^2)} \times [\Omega t \cos(\Omega t) - \sin(\Omega t)]. \quad (21)$$

Integrating the above equation over the electron transit time through the wiggler, the average change in γ_j per electron becomes

$$\langle \Delta\gamma_j \rangle_\varphi = \int_0^{T=L/v_{zj}} \left\langle \frac{d\gamma_j}{dt} \right\rangle_\varphi dt. \quad (22)$$

Substituting Eq. (21) into the above equation yields

$$\langle \Delta\gamma_j \rangle_\varphi = -\frac{eE_{rj}}{4mc} \frac{\bar{\Omega}_{wj}\beta_{zj}^2}{(\bar{\omega}_{ij}^2 - \sum_{j=1}^{2} \bar{\omega}_{bj}^2 + \beta_{zj}\sum_{j=1}^{2} \bar{\omega}_{bj}^2 \beta_{zj} - \beta_{zj}^2)} \times \frac{(ck_{wj} + \omega_{rj})D}{\Omega^3}[2 - \Omega T \sin(\Omega T) - 2\cos(\Omega T)], \quad (23)$$

where L is the FEL interaction length. The gain equation would be obtained as

$$G = \frac{\delta P}{P} = \frac{8\pi}{cE^2 \text{Area}} \frac{-mc^2}{e}[I_1\langle \Delta\gamma_1 \rangle_\varphi + I_2 \langle \Delta\gamma_2 \rangle_\varphi],$$

where $I_i = en_{bi}c\beta_{zi}\pi r_b^2$ is the average electron beam current and n_{bi} is the electron beam density, and r_{bi} is the radius of the beam. Finally, by using Eq. (23), the gain equation becomes

$$G = G_{0j} \frac{\beta_{zj}^4 F(\bar{\omega}_{ij})}{(\bar{\omega}_{ij}^2 - \sum_{j=1}^{2} \bar{\omega}_{bj}^2 + \beta_{zj}\sum_{j=1}^{2} \bar{\omega}_{bj}^2 \beta_{zj} - \beta_{zj}^2)^2}, \quad (24)$$

where

$$F(\bar{\omega}_{ij}) = 1 - \frac{\gamma_j^2 \bar{\Omega}_{wj}^2 \beta_{zj}^4 (\bar{\omega}_{ij}^2 - \sum_{j=1}^{2} \bar{\omega}_{bj}^2 + \beta_{zj}\sum_{j=1}^{2} \bar{\omega}_{bj}^2 \beta_{zj})}{2(\bar{\omega}_{ij}^2 - \sum_{j=1}^{2} \bar{\omega}_{bj}^2 + \beta_{zj}\sum_{j=1}^{2} \bar{\omega}_{bj}^2 \beta_{zj} - \beta_{zj}^2)^3 + \gamma_j^2 \bar{\Omega}_{wj}^2 \beta_{zj}^4 (\bar{\omega}_{ij}^2 - \sum_{j=1}^{2} \bar{\omega}_{bj}^2 + \beta_{zj}\sum_{j=1}^{2} \bar{\omega}_{bj}^2 \beta_{zj} - \beta_{zj}^2)},$$

and

$$G_{0j} = \frac{\bar{\omega}_{bj}^2 \bar{\Omega}_{wj}^2 f^3}{4\beta_{zj}^3 (\Omega T^3)}[2 - \Omega T \sin(\Omega T) - 2\cos(\Omega T)].$$

4. Numerical results and conclusions

A numerical study of the gain in a FEL with a planar wiggler in the presence of ion-channel guiding and self-fields has been performed. The typical dependence of the axial velocity on ion-channel frequency is obtained by using the simultaneous solution of Eqs. (7) and (8), and $\gamma_j^{-2} = 1 - \beta_{xj}^2 - \beta_{yj}^2 - \beta_{zj}^2$. The electron energy was taken to be $\gamma_1 = 3.4$ and $\gamma_2 = 3.5$, and the normalized wiggler magnetic and normalized plasma frequency of the two beams were chosen to be $\bar{\Omega}_w = 0.1$, $\bar{\omega}_{b1} = 0.4$, and $\bar{\omega}_{b2} = 0.388$, respectively.

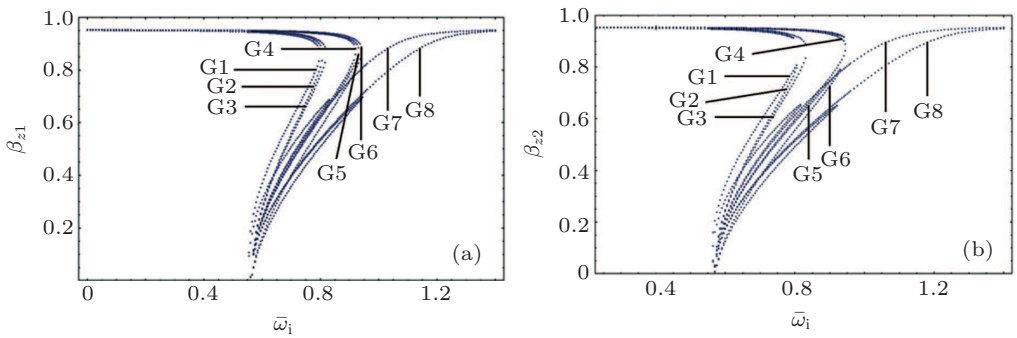


Fig. 1. (color online) Graph of the normalized axial velocity (a) β_{z1}, (b) β_{z2} of the steady-state orbits as a function of the normalized ion-channel frequency ($\bar{\omega}_i$) in the case of the two streams. The chosen parameters are $\bar{\Omega}_w = 0.1$, $\bar{\omega}_{b1} = 0.4$, and $\bar{\omega}_{b2} = 0.388$.

Figure 1(a) and 1(b) show the graph of the normalized axial velocity of the two beams, β_{z1} and β_{z2}, as a function of the normalized ion-channel frequency $\bar{\omega}_{\rm i}$. It is evident from these figures that the electron trajectories in the presence of the two streams have eight distinguished group orbits rather than the two groups reported in the absence of self-fields (Fig. 2).

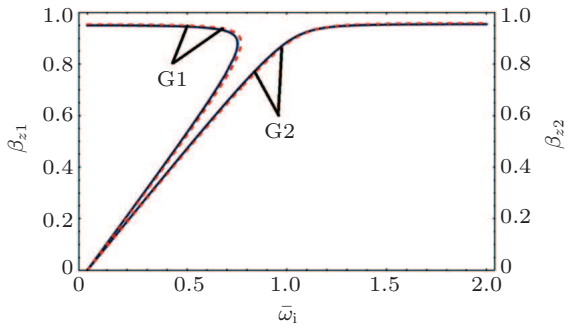


Fig. 2. (color online) Graph of the normalized axial velocity β_{z1} (solid line) and β_{z2} (dashed line) as a function of the normalized ion-channel frequency in the absence of the self-field. The chosen parameters are $\bar{\Omega}_{\rm w} = 0.1, \gamma_1 = 3.4$, and $\gamma_2 = 3.5$.

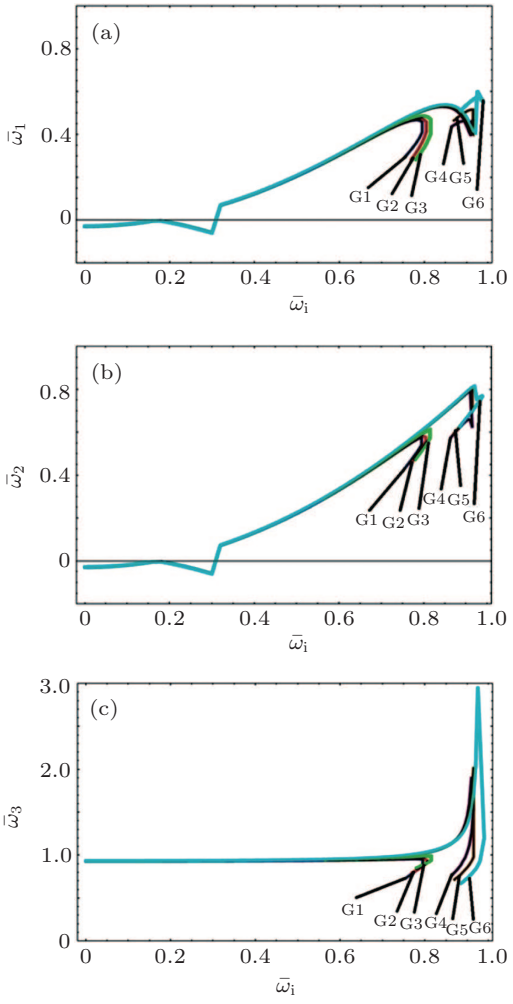


Fig. 3. (color online) (a) Graph of $\bar{\omega}_1$ versus $\bar{\omega}_{\rm i}$ corresponding to the G1–G6 orbits. (b) $\bar{\omega}_2$ versus $\bar{\omega}_{\rm i}$ corresponding to the G1–G6 orbits. (c) $\bar{\omega}_3$ versus $\bar{\omega}_{\rm i}$ corresponding to the G1–G6 orbits. The choice of system parameters are $\bar{\Omega}_{\rm w} = 0.1, \gamma_1 = 3.4$, and $\gamma_2 = 3.5$.

To investigate the stability of the steady-state two-stream electron trajectory, we find the roots of Eq. (12), namely $\bar{\omega}_1$, $\bar{\omega}_2$, and $\bar{\omega}_3$, through numerical analysis for G2–G5, G7, and G8. These groups are completely stable (Figs. 3 and 4). The obtained results for G1 and G6 indicate that these groups are not completely stable. With the aid of Figs. 3 and 4, it can be seen that these groups are stable except for the following regions: G1, $\bar{\omega}_{\rm i} < 0.31$ and $\beta_z > 0.9496$; G6, $\bar{\omega}_{\rm i} < 0.31$ and $\beta_z > 0.9523$.

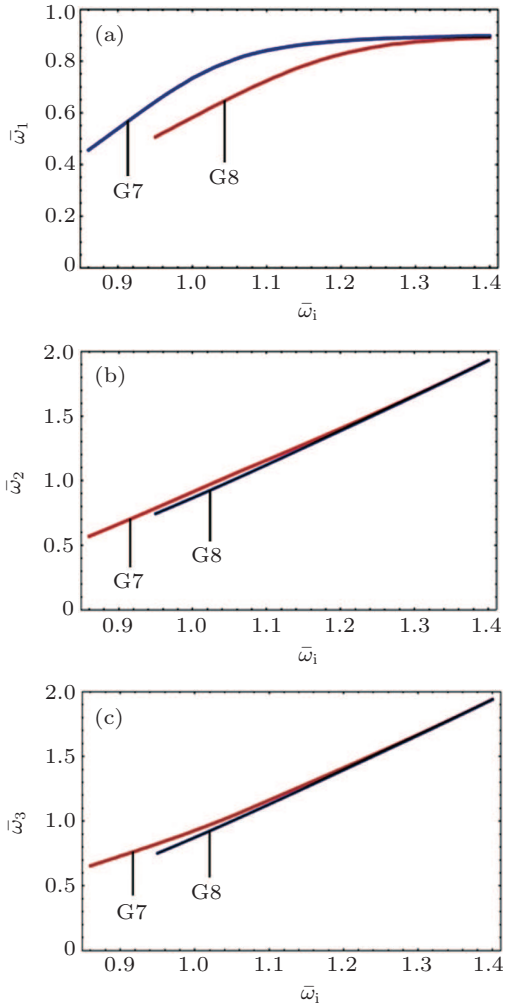


Fig. 4. (color online) (a) Graph of $\bar{\omega}_1$ versus $\bar{\omega}_{\rm i}$ corresponding to the G7 and G8 orbits. (b) $\bar{\omega}_2$ versus $\bar{\omega}_{\rm i}$ corresponding to the G7 and G8 orbits. (c) $\bar{\omega}_3$ versus $\bar{\omega}_{\rm i}$ corresponding to the G7 and G8 orbits. The choice of system parameters are $\bar{\Omega}_{\rm w} = 0.1, \gamma_1 = 3.4$, and $\gamma_2 = 3.5$.

The normalized maximum gain, $\bar{G} \equiv G_{\max}/G_0$ (the ratio of the maximum gain to the maximum gain of the planar wiggler without ion-channel guiding and self-fields), as a function of normalized ion-channel frequency is depicted in Figs. 5(a) and 5(b). The normalized gains of G1–G6 presented in Fig. 5(a) follow an increasing trend with increasing $\bar{\omega}_{\rm i}$ until they reach their asymptotic regions. The order of these normalized gains is G1 > G2 > G3 > G4 > G5 > G6. In contrast to Fig. 5(a), Figure 5(b) shows that the gain of G7 decreases with increasing $\bar{\omega}_{\rm i}$ until a minimum is reached. A further in-

crease in frequency leads to an asymptotic behavior.

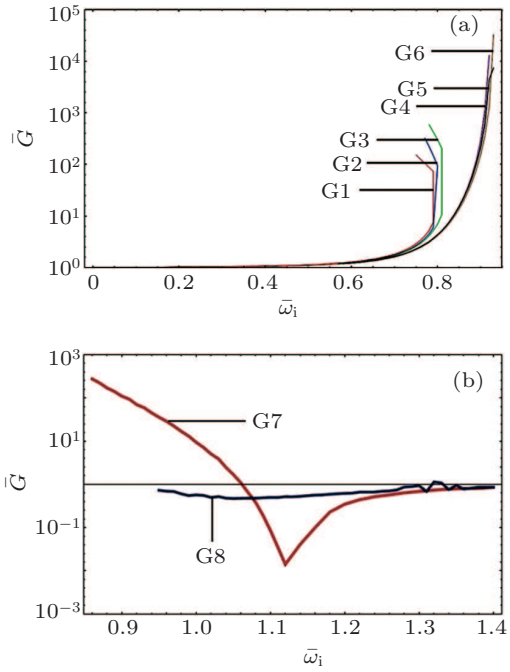


Fig. 5. (color online) Plot of the normalized maximum gain $\bar{G}$ with respect to the normalized ion-channel frequency ($\bar{\omega}_i$) for (a) G1–G6, and (b) G7 and G8. The chosen parameters are $\bar{\Omega}_w = 0.1, \gamma_1 = 3.4$, and $\gamma_2 = 3.5$.

The plot of the normalized frequency $\hat{\omega}$ corresponding to the maximum gain as a function of $\bar{\omega}_i$ is shown in Fig. 6. As shown in this figure, the order of the normalized frequency is in reverse order of that of the normalized maximum gain, and is given as $\hat{\omega}_7 > \hat{\omega}_8$ for region $1.1 < \bar{\omega}_i < 1.4$. The order of the normalized frequency for G1–G6 is $\hat{\omega}_6 > \hat{\omega}_5 > \hat{\omega}_4 > \hat{\omega}_3 > \hat{\omega}_2 > \hat{\omega}_1$.

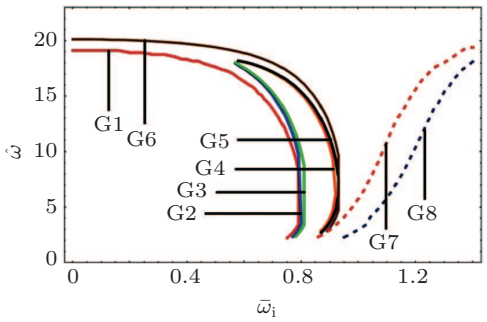


Fig. 6. (color online) Plot of the maximum normalized frequency ($\hat{\omega}$) with respect to the ion-channel frequency ($\bar{\omega}_i$) for G1–G8. The chosen parameters are $\bar{\Omega}_w = 0.1, \gamma_1 = 3.4$, and $\gamma_2 = 3.5$

The comparison between the normalized maximum gain for the two streams with and without the self-fields is given in Fig. 7(a) and 7(b). The results show that the self-fields cause the decrease in the maximum gain, with the exception of G7.

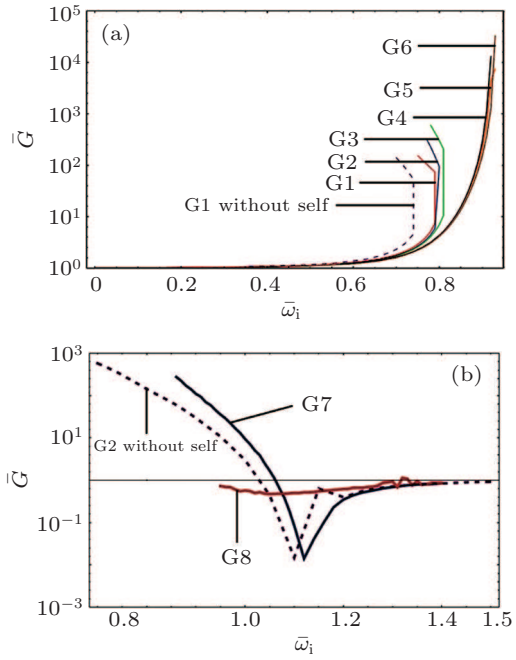


Fig. 7. (color online) (a) Graph of the normalized maximum gain $\bar{G}$ with self-field G1–G6 and without self-field (G1) as a function of the normalized ion-channel frequency $\bar{\omega}_i$. (b) Graph of the normalized maximum gain $\bar{G}$ with self-field G7 and G8 and without self-field (G2) as a function of the normalized ion-channel frequency $\bar{\omega}_i$.

Acknowledgments

This work was supported by the Plasma Physics Research Center, Science and Research Branch, Islamic Azad University.

References

[1] Roberson C W and Sprangle P 1989 *Phys. Fluids B* **1** 3
[2] Jaber I and Demokan O 1996 *Phys. Plasmas* **3** 4190
[3] Freund H P and Sprangle P 1982 *Phys. Rev A* **26** 2004
[4] Freund H P, Kehs R A and Granatstein V L 1985 *IEEE J. Quantum Electron.* **21** 1080
[5] Mehdian H, Jafari S and Hasanbeigi H 2008 *Phys. Plasmas* **15** 073102
[6] Takayama K and Hiramatsu S 1988 *Phys. Rev. A* **37** 173
[7] Seo Y, Tripathi V K and Liu C S 1989 *Phys. Fluids B* **1** 221
[8] Freund H P, Jackson R H and Pershing D E 1993 *Phys. Fluids B* **5** 2318
[9] Mirzanejhad S, Maraghechi B and Mohsenpour T 2004 *Phys. Plasmas* **11** 4777
[10] Esmaeilzadeh M, Willett J E and Willett L J 2006 *J. Plasma Phys.* **72** 59
[11] McNeil B W J, Robb G R and Poole M W 2004 *Phys. Rev. E* **70** 035501
[12] Wilhelmsson H 1991 *Phys. Scr.* **44** 603
[13] Mehdian H, Saviz S and Hasanbeigi A 2008 *Phys. Plasmas* **15** 043103
[14] Mehdian H and Saviz S 2008 *Phys. Plasmas* **15** 093103
[15] Esmaeilzadeh M, Mehdian H and Willett J E 2002 *Phys. Plasmas* **9** 670
[16] Saviz S and Mehdian H 2009 *Can. J. Phys.* **87** 1
[17] Farokhi B, Jafary F B and Maraghechi B 2006 *J. Phys. D: Appl. Phys.* **39** 3742